ReGeo ISSN: 2177-3246

TEMPORAL PATTERNS OF CLIMATE IN THE LICUNGO BASIN: A SLIDING WINDOWS APPROACH

PADRÕES TEMPORAIS DO CLIMA NA BACIA DO LICUNGO: UMA ABORDAGEM COM JANELAS DESLIZANTES

PATRONES TEMPORALES DEL CLIMA EN LA CUENCA DEL LICUNGO: UN ENFOQUE CON VENTANAS DESLIZANTES

https://doi.org/10.56238/revgeov17n7-053

Data de submissão: 25/05/2026 **Data de publicação:** 09/07/2026

Meirelles Oscar Mustafa[1], Rodrigo Nogueira de Vasconcelos[2], Nilton de Souza Ribas Júnior[3], Arleys Pereira Nunes de Castro[4], Everaldo Freitas Guedes[5], Carlos Antônio de Souza Teles Santos[6], Andréa de Almeida Brito[7], Aloisio Machado da Silva Filho[8]

ABSTRACT

The understanding of interactions among hydroclimatic variables is essential for the monitoring and sustainable management of water resources, especially in tropical regions characterized by high climatic variability. In this context, the present study aims to characterize the temporal dynamics and interrelationships among precipitation, air temperature, and streamflow in the Licungo River Basin, located in Zambézia Province, Mozambique. The analysis was conducted based on daily time series covering the period from August 1, 2002, to August 1, 2022, obtained from records of the Direção Nacional de Águas (DNA) and the Instituto Nacional de Meteorologia de Moçambique (INAM). To investigate the temporal evolution of the statistical properties of the series, a multiscale approach based on sliding windows was adopted. Initially, local descriptive statistics were estimated, allowing the assessment of changes in variability and distribution of the variables over time. Subsequently, Detrended Fluctuation Analysis (DFA) was applied to identify patterns of memory and long-range persistence in the series. The dependence between variables was investigated using Detrended Cross-Correlation Analysis (DCCA), including the coefficient [EQUAÇÃO 1] to evaluate bivariate correlations across different time scales. Additionally, the Detrended Multiple Cross-correlation coefficient ([EQUAÇÃO 2]) was employed, enabling the analysis of joint dependence among hydroclimatic variables. Finally, the complexity and predictive potential of the series were evaluated using normalized entropy

[1] Doutorando. Universidade Federal do Rio Grande do Sul. E-mail: mireloscar@gmail.com
Orcid: https://orcid.org/0009-0004-4590-0317
[2] Doutor. Universidade Estadual de Feira de Santana (UEFS). E-mail: rnvasconcelos@uefs.br
Orcid: https://orcid.org/0000-0002-1368-6721
[3] Doutor. Instituto Brasileiro de Geografia e Estatística (IBGE). E-mail: niltonribasjr@gmail.com
Orcid: https://orcid.org/0000-0003-2170-136X
[4] Doutor. Fundação Visconde de Cairu (FVC). E-mail: arleys.castro@gmail.com
Orcid: https://orcid.org/0000-0001-8221-4843
[5] Doutor. Fundação Oswaldo Cruz (Fiocruz). E-mail: efgestatistico@gmail.com
Orcid: https://orcid.org/0000-0002-2986-7367
[6] Doutor. Fundação Oswaldo Cruz (Fiocruz). E-mail: carlos.teles@fiocruz.br
Orcid: https://orcid.org/0000-0003-0970-0479
[7] Doutora. Instituto Federal de Educação, Ciência e Tecnologia (IFBA). E-mail: britodea@gmail.com
Orcid: https://orcid.org/0000-0002-7644-2919
[8] Doutor. Universidade Estadual de Feira de Santana (UEFS). E-mail: aloisioestatistico@uefs.br
Orcid: https://orcid.org/0000-0001-8250-1527

(FastApEn). The results reveal the presence of persistent patterns, multiscale variability, and cross-dependencies among precipitation, temperature, and streamflow, highlighting the importance of an integrated analysis of these variables to better understand the hydroclimatological behavior of the basin. The adopted approach contributes to the improvement of hydrometeorological monitoring and provides relevant scientific support for planning and water resource management in regions subject to high climatic variability.

Keywords: Time Series. Sliding Windows. DFA. DCCA. Entropy. Hydroclimatic Variability.

RESUMO

A compreensão das interações entre as variáveis hidroclimáticas é essencial para o monitoramento e a gestão sustentável dos recursos hídricos, especialmente em regiões tropicais caracterizadas por elevada variabilidade climática. Este estudo teve como objetivo caracterizar a dinâmica temporal e as inter-relações entre precipitação, temperatura do ar e vazão na Bacia do Rio Licungo, localizada na província da Zambézia, Moçambique. Foram analisadas séries temporais diárias referentes ao período de 1º de agosto de 2002 a 1º de agosto de 2022, obtidas junto à Direção Nacional de Águas (DNA) e ao Instituto Nacional de Meteorologia de Moçambique (INAM). Adotou-se uma abordagem multiescala baseada em janelas deslizantes, utilizando estatísticas descritivas locais, Análise de Flutuação sem tendência (DFA), Coeficiente de Correlação Cruzada sem tendência [EQUAÇÃO 5] Coeficiente de correlação cruzada múltipla sem tendência ([EQUAÇÃO 6]) e entropia aproximada normalizada (FastApEn). Os resultados evidenciaram padrões persistentes, variabilidade multiescala e dependências cruzadas entre precipitação, temperatura e vazão, indicando que a precipitação exerce papel dominante na dinâmica hidrológica, enquanto a temperatura atua como variável moduladora. A abordagem proposta amplia a compreensão do comportamento hidroclimatológico da bacia e fornece subsídios para o monitoramento hidrometeorológico, a modelagem hidrológica e a gestão de recursos hídricos em regiões sujeitas à elevada variabilidade climática.

Palavras-chave: Séries Temporais. Janelas Deslizantes. DFA. DCCA. Entropia. Variabilidade Hidroclimática.

RESUMEN

La comprensión de las interacciones entre las variables hidroclimáticas es esencial para el monitoreo y la gestión sostenible de los recursos hídricos, especialmente en regiones tropicales caracterizadas por una alta variabilidad climática. En este contexto, el presente estudio tuvo como objetivo caracterizar la dinámica temporal y las interrelaciones entre la precipitación, la temperatura del aire y el caudal en la cuenca del río Licungo, ubicada en la provincia de Zambézia, Mozambique. El análisis se realizó a partir de series temporales diarias correspondientes al período comprendido entre el 1 de agosto de 2002 y el 1 de agosto de 2022, obtenidas de la Direção Nacional de Águas (DNA) y del Instituto Nacional de Meteorologia de Moçambique (INAM). Para investigar la evolución temporal de las propiedades estadísticas de las series se adoptó un enfoque multiescala basado en ventanas deslizantes. Inicialmente se estimaron estadísticas descriptivas locales para evaluar los cambios en la variabilidad y la distribución de las variables a lo largo del tiempo. Posteriormente se aplicó el Análisis de Fluctuación sin Tendencia (DFA) para identificar patrones de memoria y persistencia de largo alcance. La dependencia entre las variables se investigó mediante el Análisis de Correlación Cruzada sin Tendencia (DCCA), incluyendo el coeficiente [EQUAÇÃO 3] para evaluar correlaciones bivariadas en diferentes escalas temporales. Además, se empleó el coeficiente de correlación cruzada múltiple sin tendencia ([EQUAÇÃO 4]), lo que permitió analizar la dependencia conjunta entre las variables

hidroclimáticas. Finalmente, la complejidad y el potencial predictivo de las series se evaluaron mediante la entropía normalizada (FastApEn). Los resultados revelaron la presencia de patrones persistentes, variabilidad multiescala y dependencias cruzadas entre la precipitación, la temperatura y el caudal, destacando la importancia de un análisis integrado para comprender mejor el comportamiento hidroclimatológico de la cuenca. El enfoque adoptado contribuye al fortalecimiento del monitoreo hidrometeorológico y proporciona un soporte científico relevante para la planificación y la gestión de los recursos hídricos en regiones sujetas a una elevada variabilidad climática.

Palabras clave: Series Temporales. Ventanas Deslizantes. DFA. DCCA. Entropía. Variabilidad Hidroclimática.

1 INTRODUCTION

Climate change has intensified pressures on water resources, widening the gap between water supply and demand, particularly in vulnerable regions where population growth, urbanization, and land-use changes exacerbate the effects of climate variability (Droogers; Bouma, 2014; Erler *et al.*, 2019; Juizo; Liden, 2010). Although global trends are widely documented, studies indicate that climatic and hydrological responses exhibit strong regional heterogeneity, requiring analyses at the local scale (Hartmann, 2013).

The spatiotemporal variability of water availability represents a critical challenge for water planning and sustainable management, particularly in African countries. In Mozambique, this issue is intensified by limited monitoring infrastructure: only about 60% of hydrometeorological stations are operational, and fewer than 20% perform streamflow measurements, significantly restricting hydrological assessment capacity (DNGRH, 2014). This limitation compromises flood and drought forecasting and hinders the development of effective adaptation strategies.

In this context, the Licungo River Basin, located in Zambézia Province, plays a fundamental role in domestic water supply, agriculture, and the maintenance of local ecosystems. However, the region is frequently affected by extreme events, such as floods and drought periods, associated with the high rainfall irregularity typical of tropical climates (Muchangos, 1999). This hydroclimatic variability generates substantial uncertainty for water resource management, further exacerbated by the scarcity of systematic studies that integrate precipitation, temperature, and streamflow from a temporal and multiscale perspective.

Isolated analyses of hydrological variables are generally insufficient to understand the response of river basins to climate change, since hydrological behavior results from the interaction among multiple physical and climatic processes (Köplin *et al.*, 2012; Viviroli *et al.*, 2011). In this context, methods based on the analysis of non-stationary time series have been widely used to investigate the dynamic properties of complex environmental systems. Among these methods, *Detrended Fluctuation Analysis* (DFA) (Peng *et al.*, 1994) and detrended cross-correlation coefficients, such as DCCA (G. Figueira. Zebende, 2011) and DMC (Zebende & Silva–Filho., 2018), stand out as particularly effective in identifying long-term persistence and cross-dependencies between variables across different time scales (Brito *et al.*, 2019; Doria *et al.*, 2025; Ribas Junior *et al.*, 2025, 2026; Toledo *et al.*, 2022). Despite

recent advances, the application of these approaches remains limited in the hydroclimatological context of Mozambique.

In addition, information-theoretic approaches, such as entropy, have been employed to characterize predictability and complexity in environmental systems, providing relevant support for hydrological monitoring and decision-making in data-scarce regions (Ilunga, 2017, 2019). Recent studies in African basins also demonstrate that climate variability directly affects water resilience and food security, reinforcing the need for detailed local-scale assessments (Hakam *et al.*, 2024; Tibangayuka *et al.*, 2025).

In this context, the present study aims to characterize the temporal dynamics and interrelationships among precipitation, temperature, and streamflow in the Licungo River Basin over the period from 2002 to 2022. To this end, an integrated approach is adopted based on the application of time series analysis methods with sliding windows including descriptive statistics, Detrended Fluctuation Analysis (DFA), and detrended bivariate cross-correlation $\rho_{DCCA}(n)$ (G. Figueira. Zebende, 2011) and multiple $DMC_x^2(n)$ (Zebende & Silva–Filho., 2018) in addition to normalized approximate entropy (FASTApEn) (Tomčala, 2018), estimated as a function of different time scales. This approach enables the investigation of the temporal evolution of the statistical properties of the series and the identification of patterns of persistence, cross-dependence, and predictability over time, contributing to a better understanding of the hydroclimatic behavior of the basin.

The use of sliding windows in time series analysis allows tracking the temporal evolution of the statistical properties of the series, overcoming limitations of methods based on fixed periods (Doria *et al.*, 2025; Guedes *et al.*, 2021; Ribas Junior *et al.*, 2025; Santos *et al.*, 2022; Silva Filho *et al.*, 2021). This approach enables the identification of abrupt changes associated with extreme events or different climatic regimes, contributing to the improvement of hydrometeorological monitoring, hydrological model calibration, and integrated water resource management in regions subject to high climatic variability, such as the study area of this research.

To achieve the objective of this article, it is organized into five sections: Introduction 1; Materials and Methods, where the study area, its climatic and environmental characteristics, and the methods that underpin the results are presented 2; Results and Discussion 4; Research Limitations 5; and, finally, Conclusions 6.

2 MATERIALS AND METHODS

2.1 STUDY AREA

The Licungo River Basin (LRB) is located in Zambézia Province, Mozambique, between latitudes 15 ❑° 18'–17 ❑° 42' South and longitudes 35 ❑° 45'–37 ❑° 33' East. The Licungo River originates in the Namúli Mountains, near the city of Gurué, at approximately 1650 m of altitude, and flows for about 336 km before discharging into the Indian Ocean, near Vila Valdez, approximately 50 km north of the city of Quelimane. The basin covers an area of approximately 27,726 km ❑^{2} and exhibits a pronounced altimetric gradient between the upstream and downstream sectors, a characteristic that directly influences hydrological dynamics and river flow. In addition, the region presents significant geological diversity and the occurrence of mineral resources, aspects that contribute to the environmental complexity of the hydrographic system (Muchangos, 1999).

Hydrological monitoring of the basin is carried out through hydrometric stations distributed along the drainage network. Among these stations, station E91 (see Figure 1), located at Mocuba Bridge, stands out and was selected in this study as the main analysis point due to the greater availability and continuity of hydrometeorological series. The strategic location of this station in the middle-lower reach of the river allows the integration of hydrological contributions from different sectors of the basin and is also an area historically susceptible to flooding events. The coordinates of the main hydrometric stations considered in the basin are presented in Table 1.

Table 1

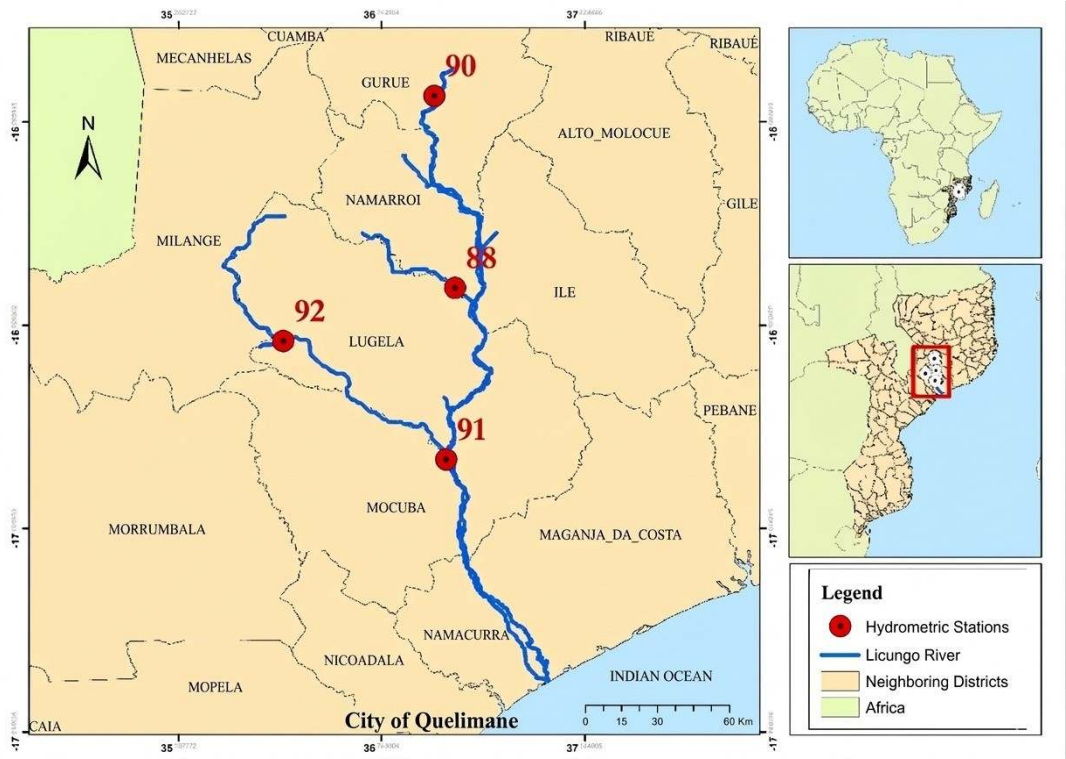
Coordinates of hydrometric stations in the Licungo River Basin

Station	Location	Latitude (S)	Longitude (E)	Altitude (m)
88	Luo in Mocubi	16❑°11’05”	37❑°01’09”	330
90	Licungo at EN231 Gurué	15❑°28’00”	36❑°56’30”	650
91	Licungo at Mocuba Bridge	16❑°49’33”	36❑°59’09”	100
92	Lugela at Tacuane	16❑°23’00”	36❑°22’30”	260

Source: DNA.

Figure 1

Location of the Licungo River Basin in Mozambique and spatial distribution of the hydrometric stations used in this study. The main panel shows the Licungo River drainage network and the positions of the monitoring stations (88, 90, 91 and 92). The inset maps indicate the location of the basin within Mozambique and the African continent



Source: Prepared by the authors.

2.2 PHYSIOGRAPHIC AND CLIMATIC CHARACTERIZATION

The Licungo River Basin exhibits significant physiographic diversity, resulting from altimetric variation and the geological characteristics of the region. The relief ranges approximately between 233 and 3127 meters in elevation, encompassing mountainous areas in the headwater regions and extensive plains in the lower portions of the basin. This topographic heterogeneity directly influences hydrological processes, conditioning surface runoff dynamics and the organization of the drainage network. From a geological perspective, Precambrian formations predominate, mainly composed of metamorphic rocks such as gneisses and migmatites, which form the structural basement of the region and exert a strong influence on landscape morphology and the evolution of the fluvial system (Muchangos, 1999).

In climatic terms, the basin is located in a tropical region characterized by strong rainfall seasonality. The rainy season is concentrated mainly between November and March,

accounting for most of the annual precipitation, while the remaining months present relatively drier conditions. The mean annual precipitation ranges approximately between 1000 and 2000 millimeters, with spatial distribution influenced by topography and proximity to the Indian Ocean. Mean annual temperatures show moderate variation, generally ranging between 19 and 30 °C. Regarding land use and land cover, areas dedicated to subsistence agriculture predominate, interspersed with natural forest formations and shrub vegetation, highlighting the socioeconomic importance of the basin for local populations.

2.3 DATA BASE

The analyzed period spans 20 years, from August 1, 2002, to August 1, 2022, with daily data for three hydroclimatic variables: streamflow (m^3/s), mean air temperature (°C), and precipitation (mm). The data were obtained from records of the National Directorate of Water of Mozambique (DNA) and the National Institute of Meteorology (INAM), and were complemented with international datasets. All series were subjected to quality control procedures, including temporal consistency checks and cross-validation among different data sources.

For the temporal analyses, hydrometric station E91 was selected due to the greater continuity and quality of the available historical series. Missing values were treated using imputation procedures implemented in the *R* language, employing the zoo, imputeTS, and forecast packages. Interpolation and temporal reconstruction techniques suitable for non-stationary environmental series were applied (Pereira *et al.*, 2024).

2.4 DEPENDENCE AND COMPLEXITY IN TIME SERIES

2.4.1 DFA - dentreded fluctuation analysis

Detrended Fluctuation Analysis (DFA), proposed by (Peng *et al.*, 1994), is a widely used method to identify and quantify long-range autocorrelations in non-stationary time series. The procedure initially consists of integrating the time series x_i, with $i=1,\ldots,N$, after removing the mean, yielding the accumulated series X_K. Subsequently, the integrated series is divided into segments of size n (time scale), in which a local trend is fitted, typically using a polynomial of degree greater than or equal to 1.

From the difference between the integrated series and the fitted trend in each segment, the local variance of the fluctuations is calculated. The global fluctuation function is then defined as

$$F_{DFA}(n)=\sqrt{\frac{1}{N-n}\sum_{i=1}^{N-n} f_{DFA}^{2}(n,i)}, \quad (1)$$

where n is the time scale and N is the length of the series. This procedure is repeated for different scales n, typically within the range $4 \le n \le N/4$. If the relationship between $F_{DFA}(n)$ and n follows a power law, $F_{DFA}(n) \sim n^{\alpha_{DFA}}$, the exponent α_{DFA} characterizes the degree of temporal correlation in the series. The values of the exponent α_{DFA} allow the interpretation of the time series behavior: values $\alpha < 0.5$ indicate antipersistent behavior, $\alpha \approx 0.5$ corresponds to white noise, $0.5 < \alpha < 1$ indicates long-range persistence, while $\alpha \approx 1.5$ is associated with Brownian noise (Zebende *et al.*, 2016).

2.4.2 DCCA and the ρ coefficient

Detrended Cross-Correlation Analysis (DCCA), proposed by (Podobnik; Stanley, 2008), is an extension of the DFA method and aims to identify long-range correlations between two possibly non-stationary time series, xi and yi. The method is initially based on integrating the series after removing their means, generating the accumulated series Xk and Yk Subsequently, these series are divided into segments of size *n* (time scale), in which a local trend is fitted using polynomials. After removing these trends, the covariance of the residuals is computed in each segment, and its average provides the cross-fluctuation function FDCCA(*n*). If the relationship between FDCCA(*n*). and the time scale *n* follows a power law, F2DCCA(*n*) ~ n2DCCA., the exponent DCCA characterizes the degree of long-range cross-correlation between the series. Based on this procedure, (G. Figueira. Zebende, 2011) proposed the detrended cross-correlation coefficient $\rho_{DCCA}(n)$, which quantifies the level of dependence between two non-stationary time series. This coefficient is defined as

$$\rho_{DCCA}(n)=\frac{F_{DCCA}^{2}(n)}{F_{DFA-X}(n)F_{DFA-Y}(n)}, \quad (2)$$

where $F_{DFA-X}(n)$ and $F_{DFA-Y}(n)$ correspond to the fluctuation functions obtained by the DFA method for each individual series. The coefficient takes values in the interval $-1 \le \rho_{DCCA} \le 1$, indicating, respectively, perfect anti-correlation, absence of correlation, and perfect cross-correlation between the analyzed series.

2.4.3 Multiple cross-correlation coefficient ρDMC

The detrended multiple cross-correlation coefficient, DMC_X^2, proposed by (Zebende & Silva–Filho., 2018), constitutes a generalization of the ρ_{DCCA} coefficient and aims to quantify the joint correlation between a dependent variable and two or more possibly non-stationary time series. The coefficient is defined as

$$\mathrm{DMC}_x^2(n)=\rho_{y,x_i}(n)^T\rho^{-1}(n)\rho_{y,x_i}(n), \tag{3}$$

where $\rho_{y,x_i}(n)$ represents the vector of cross-correlations between the dependent variable y and the independent variables x_i, while $\rho^{-1}(n)$ corresponds to the inverse matrix of cross-correlations among the independent variables.

The coefficient takes values in the interval $0\leq DMC_x^2(n)\leq 1$, where values close to 1 indicate strong multiple correlation among the analyzed series, while values close to 0 indicate weak joint dependence. For the interpretation of DMC_x^2, consider the table below, according to (Silva Filho *et al.*, 2026; Zebende & Silva–Filho., 2018).

Table 2

Intervals of detrended multiple cross-correlation coefficients

Levels	$DMC_x^2(n)$
Very weak	$0.0-0.2$
weak	$0.2-0,4$
Moderate	$0.4-0.6$
Strong	$0.6-0.8$
Very strong	$0.8-1.0$

Source: Prepared by the authors.

2.4.4 Sliding windows

The sliding window technique is widely used in the analysis of non-stationary time series, allowing the investigation of the temporal evolution of local statistical properties. Consider a time series $x_{tt=1}^{N}$. The method consists of partitioning the series into overlapping subsets of fixed length w, shifted over time (Guedes *et al.*, 2021; Ribas Junior *et al.*, 2025; Silva Filho *et al.*, 2021). For each position τ, the window is defined as

$$X_\tau=\{x_\tau,x_{\tau+1},\ldots,x_{\tau+w-1}\}, \tag{4}$$

with $\tau=1,2,\ldots,N_w$, where the total number of windows is given by

$$N_w = N - w + 1. \quad (5)$$

In each window, local statistics or measures of temporal dependence are computed, allowing the tracking of the series dynamics over time (Guedes *et al.*, 2021; Silva Filho *et al.*, 2021). In general, a local statistic can be represented as

$$\Theta(\tau) = F\left(x_\tau, x_{\tau+1}, \ldots, x_{\tau+w-1}\right), \quad (6)$$

where $F(\cdot)$ represents a statistical operator, such as the mean, standard deviation, DFA exponent, or cross-correlation coefficients (Doria *et al.*, 2025).

In the case of descriptive statistics, the most commonly used local measures include the mean

$$\mu(\tau) = \frac{1}{w}\sum_{i=0}^{w-1} x_{\tau+i}, \quad (7)$$

and the standard deviation

$$\sigma(\tau) = \sqrt{\frac{1}{w}\sum_{i=0}^{w-1}\left(x_{\tau+i} - \mu(\tau)\right)^2}. \quad (8)$$

The approach can also be integrated with methods for analyzing temporal dependence, such as DFA and Detrended Cross-Correlation Analysis (DCCA), enabling the dynamic estimation of the autocorrelation exponent $\alpha(\tau)$ and the cross-correlation coefficient $\rho_{DCCA}(n,\tau)$ across different time scales (Costa *et al.*, 2019; Guedes *et al.*, 2021; Santos *et al.*, 2022). In this way, the technique allows the identification of changes in the persistence of the series and in the intensity of correlations over time.

In this study, a sliding window size of 365 days ($w = 365$) was adopted, as suggested by (Santos *et al.*, 2022) and (Doria *et al.*, 2025). This length represents an appropriate trade-off between statistical stability and temporal resolution, allowing the capture of the full annual cycle of the analyzed hydroclimatic variables.

2.4.5 Entropy

Entropy is a fundamental measure from Information Theory that quantifies the degree of uncertainty or complexity associated with a random variable (Shannon, 1948). In the

context of time series, this measure is used to evaluate the level of predictability and the structure of data over time (Ribas Junior *et al.*, 2026). More regular and predictable series tend to exhibit lower entropy values, whereas series with greater randomness or complexity present higher values (Pincus, 1991).

In this study, the *Approximate Entropy* (ApEn) measure, proposed by (Pincus, 1991), was used. It quantifies the regularity and complexity of a time series by evaluating the probability that similar patterns of length m remain similar when a new point is added to the sequence. Let $x_1, x_2, \ldots, x_N$ be a time series of length N. The approximate entropy is defined as

$$ApEn(m, r, N) = \phi^m(r) - \phi^{m+1}(r), \tag{9}$$

where m represents the embedding dimension, r is the tolerance parameter (typically defined as a fraction of the standard deviation of the series), and N corresponds to the length of the analyzed series.

To optimize computational cost, especially in analyses based on sliding windows, the optimized version known as *Fast Approximate Entropy* (FastApEn), proposed by (Tomčala, 2018), was used. This approach preserves the principles of ApEn but employs more efficient computational strategies to accelerate calculations for large data volumes.

For comparison purposes among different windows or time series, the entropy values were normalized within the interval $[0, 1]$, as shown in the expression below (Ribas Junior *et al.*, 2026):

$$\text{Normalized Entropy} = \frac{x - min(x)}{max(x) - min(x)}. \tag{10}$$

where x represents the value of the entropy measure for a given window or time series, $min(x)$ corresponds to the lowest entropy value observed in the analyzed dataset, and $max(x)$ indicates the highest entropy value observed in the analyzed dataset.

Values close to zero indicate higher predictability and greater regularity in the behavior of the time series, whereas values close to one indicate greater complexity or randomness in the system (Ribas Junior *et al.*, 2026). In this study, entropy was calculated as a function of the time scale (n, in days), allowing the identification of intervals of n in which the system

exhibits higher or lower levels of complexity, reflecting different degrees of predictability in the analyzed time series.

Applications of entropy in time series are broad and interdisciplinary. In physiology, this measure is used to analyze the variability of biological signals, such as heart rate, respiration, and electroencephalography (Pincus, 1991; Richman; Moorman, 2000). In climatology and hydrology, entropy has been employed to characterize the variability of hydroclimatic variables, such as precipitation, temperature, streamflow, and soil moisture, enabling the assessment of the complexity and predictability of environmental systems (Li, 2018; Singh, 2013). In addition, applications include signal engineering for fault detection and noise identification (Azami, 2016), as well as fields such as finance, ecology, and environmental sciences, in which entropy assists in evaluating uncertainty, volatility, and stability in complex systems (Kapur; Kesavan, 1992; Liang, 2020).

In the subsequent section, the main results of this study are presented and discussed, obtained from the analysis of different properties of the time series. These results allow for a better understanding of the hydroclimatological behavior of the basin under study and its implications for water resource management.

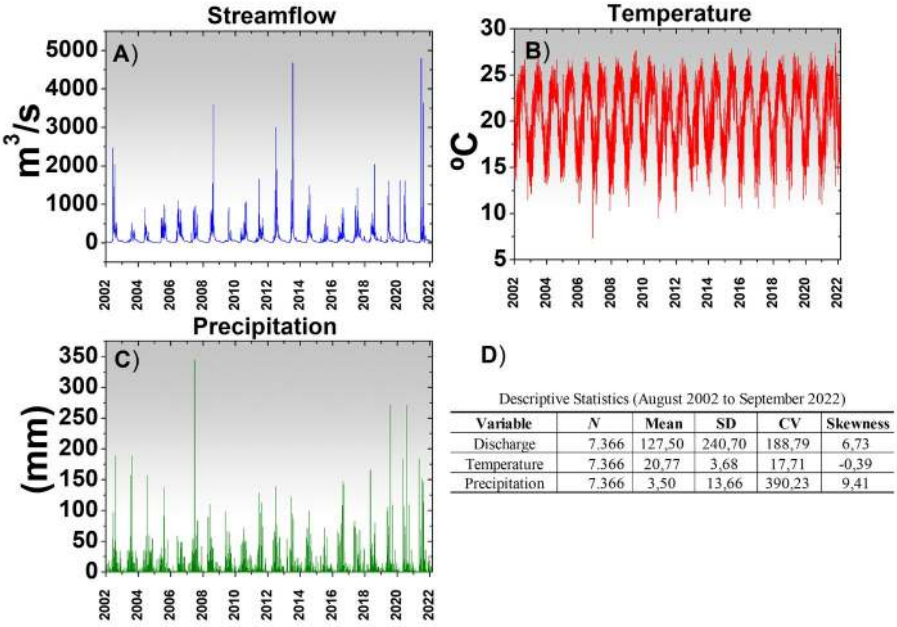
3 RESULTS AND DISCUSSION

3.1 EXPLORATORY DATA ANALYSIS

Figure 2 presents an integrated view of the fluctuation behavior of the hydroclimatic time series in the Licungo Basin over the period from 2002 to 2022 ($N = 7,366$ points), allowing the identification of temporal patterns and relevant statistical characteristics.

Figure 2

Original time series of discharge, temperature, and precipitation in the Licungo River Basin from 2002 to 2022



Descriptive Statistics (August 2002 to September 2022)

Variable	*N*	Mean	SD	CV	Skewness
Discharge	7.366	127,50	240,70	188,79	6,73
Temperature	7.366	20,77	3,68	17,71	-0,39
Precipitation	7.366	3,50	13,66	390,23	9,41

Notes: A: Streamflow B: Temperature C: Precipitation D: Descriptive statistics of the variables. In figure D, N denotes the size of the series, SD - Standard deviation, CV - Coefficient of variation. The x-axis represents time (days across the years), while the y-axis shows the variability of the analyzed variables.
Source: Prepared by the authors.

In the streamflow series (Figure 2-A), pronounced interannual variability is observed, with marked flood peaks in specific years associated with extreme precipitation events. Statistical analysis indicates that the streamflow distribution is strongly positively skewed (Sk = 6.73), highlighting the predominance of low values interspersed with sporadic occurrences of intense floods. These extreme events are consistent with historical records widely documented for the Licungo River Basin, notably the floods of January 2015, resulting from intense precipitation in the region (International Federation of Red Cross and Red Crescent Societies, 2015; NASA Earth Observatory, 2015), and the impacts associated with Cyclone Idai in March 2019, which caused widespread flooding in Zambézia Province, including the Licungo Basin (ACAPS, 2019). A recent hydrological study identified the years 2014, 2015, 2019, and 2022 as periods of historical floods in the basin, highlighting the association between observed streamflow peaks and extreme climatic events (Cea *et al.*, 2022).

In contrast to the high variability observed in streamflow, air temperature (Figure 2-B) exhibits a more stable behavior over the analyzed period, a characteristic typical of tropical regions, where climatic seasonality is predominantly controlled by precipitation and large-

scale atmospheric circulation. As reported by (New *et al.*, 2002), mean temperature in these regions tends to show low annual thermal amplitude, resulting in relatively uniform behavior over time. This pattern is also evident in the exploratory data analysis, in which the coefficient of variation presents a moderate value (CV = 17.71%), indicating low relative dispersion of temperature values.

Similarly to streamflow, precipitation (Figure 2-C) exhibits high variability, but with characteristics typical of tropical regimes, being marked by strong temporal irregularity, with intense events concentrated during the rainy season and prolonged dry periods (Cea *et al.*, 2022). The extremely high coefficient of variation (CV = 390.2%) reflects this dynamic, typical of regions where rainfall is concentrated in a few intense events interspersed with long dry periods. The high skewness of the distribution (Sk = 9.41) reinforces this interpretation, indicating the presence of extreme values associated with intense precipitation events.

Taken together, these results highlight the complexity and high variability of the analyzed hydroclimatic series, especially in basins located in tropical regions. Similar findings have been reported in studies conducted in African basins, where the high spatial and temporal uncertainty of hydrological data has motivated the use of information-theoretic metrics, such as entropy, to better characterize variability and support monitoring and water resource management decisions (Ilunga, 2017, 2019).

3.2 DESCRIPTIVE STATISTICS USING SLIDING WINDOW

The analysis of hydroclimatic variables using sliding windows (Figure 3) reveals distinct patterns of variability and distribution over the analyzed period. Streamflow (Figure 3-A) exhibits high temporal variability, with recurrent peaks associated with more intense hydrological events, particularly in years such as 2008, 2011, 2015, and 2019. This behavior is reinforced by the high values of the coefficient of variation (Figure 3-B), frequently exceeding 200%, indicating strong instability in the hydrological regime. The positive skewness (Figure 3-C) during periods of higher streamflow suggests right-skewed distributions, associated with the occurrence of extreme events, with values significantly above the mean.

In contrast to the high variability of streamflow, air temperature (Figure 3-D) exhibits a more stable behavior, with smooth variations over time and indications of a slight increase, particularly after 2015. The values of the coefficient of variation (Figure 3-E) remain relatively constant, generally between 16% and 19%, indicating low relative dispersion. The skewness

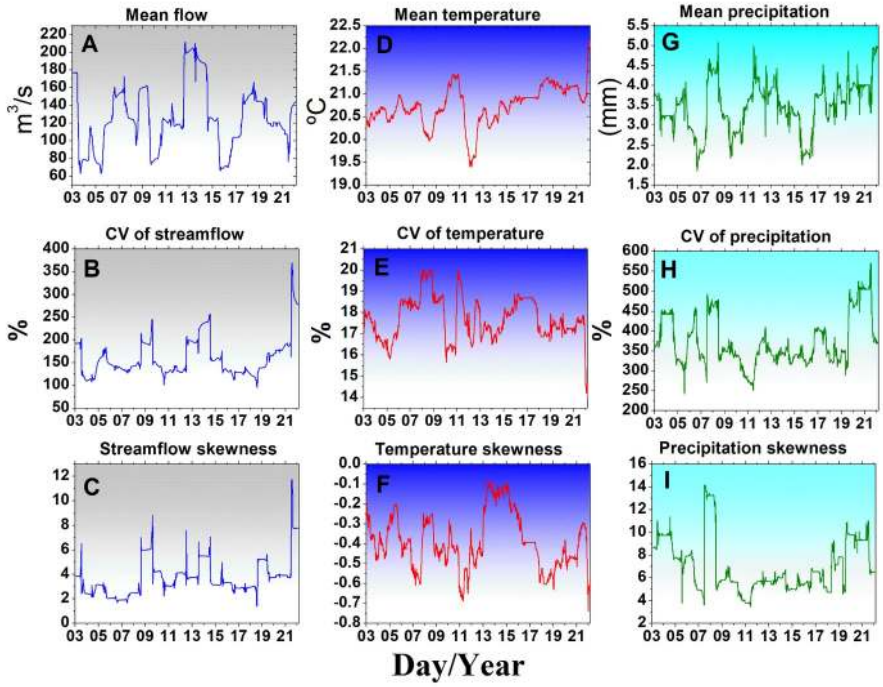
(Figure 3-F) shows smaller amplitude compared to the other variables, suggesting a more balanced distribution and lower influence of extreme values, a characteristic typical of tropical regions (New *et al.*, 2002).

Similarly to streamflow, precipitation (Figure 3-G) exhibits highly irregular behavior, with the occurrence of intense peaks distributed non-uniformly over time. The coefficient of variation (Figure 3-H) remains at extremely high levels, around 400%, with more pronounced increases in years such as 2006, 2009, 2014, and 2021, as well as greater variability after 2017, reflecting the typical irregularity of tropical regions (Cea *et al.*, 2022). The skewness (Figure 3-I) frequently exceeds 10, with peaks during the periods 2003–2005 and 2020–2022, indicating strongly right-skewed distributions associated with the occurrence of extreme precipitation events, characterized by high and infrequent values concentrated over short time intervals.

Overall, the results obtained through the sliding window analysis are consistent with those identified in the exploratory analysis, highlighting the robustness of the observed hydroclimatic patterns. However, the sliding approach provides an additional level of detail by capturing local temporal variations in variability and distribution shape, offering a more refined understanding of the dynamics of the series over time.

Figure 3

Sliding descriptive statistics (mean, coefficient of variation, and skewness) of the Licungo River Basin from 2002 to 2022



Note: The descriptive statistics were computed using $w = 365$ days.
Source: Prepared by the authors.

The results obtained so far, based on the exploratory analysis (Section 4.1) and the descriptive statistics using sliding windows (Section 4.2), highlight the complexity and non-stationarity of the analyzed series, emphasizing the need for methods capable of adequately assessing temporal dependence and predictability across multiple scales, as presented in the following sections. In this context, a study conducted in another African basin indicates that this spatiotemporal variability can be explored through approaches that combine entropy, kriging, and multicriteria decision methods, enabling the optimization of monitoring networks and the prioritization of locations that maximize hydrological information gain (Tekleyohannes *et al.*, 2021).

3.3 SLIDING DFA

Figure 4 presents the temporal evolution of the autocorrelation exponent α_{DFA}, estimated using the sliding window approach based on the DFA (Detrended Fluctuation

Analysis) method, applied to the streamflow (Figure 4-A), temperature (Figure 4-C), and precipitation (Figure 4-E) series, as well as their respective histograms (Figure 4-B, D, and F).

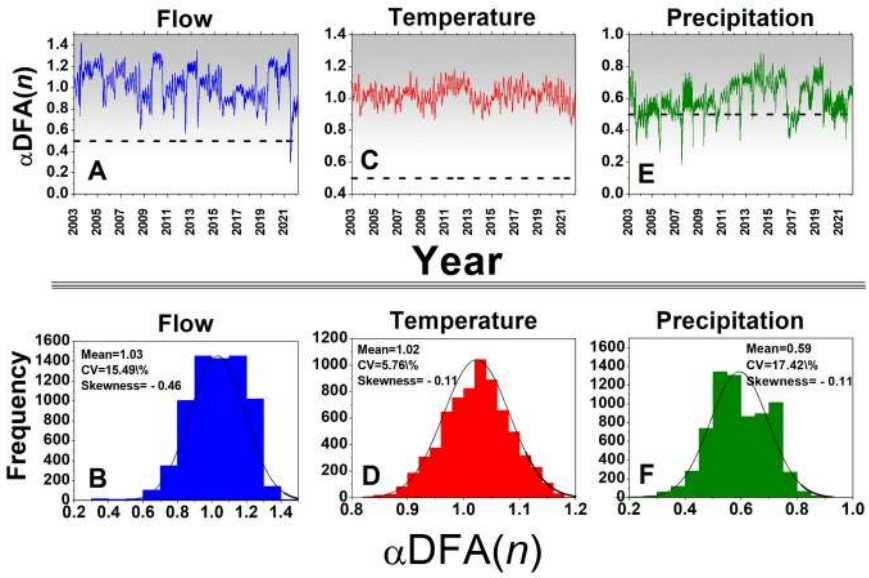
Streamflow exhibits α_{DFA} values ranging from 0.30 to 1.43, with a mean of 1.03, characterizing a persistently correlated regime and evidencing long-range hydrological memory. This behavior suggests that periods of higher discharge tend to be followed by similar conditions, reflecting cumulative processes within the basin. Similar results were reported by (Toledo *et al.*, 2022), who found a mean value of the exponent α close to 0.91 in streamflow series, also associated with persistence and temporal dependence across multiple scales.

Temperature exhibits greater regularity, with α_{DFA} ranging between 0.9 and 1.1 and a mean of 1.02, indicating high persistence and strong temporal dependence. This pattern is consistent with the more stable nature of this variable, associated with well-defined seasonal cycles and reduced interannual variability typical of tropical regions. In contrast, precipitation presents mean values around 0.59, indicating weaker persistence compared to the other variables. This characteristic is related to the intermittent nature of rainfall, marked by high variability and greater influence of stochastic processes.

The histograms corroborate these findings. For streamflow (Figure 4-B), a mean of 1.03, a coefficient of variation of 15.49%, and negative skewness (-0.46) are observed, suggesting the predominance of persistent values with occasional episodes of lower temporal dependence. Temperature (Figure 4-D) presents a mean of 1.02, low variability (CV = 5.76%), and an approximately symmetric distribution (skewness = -0.11), reinforcing its stability. In contrast, precipitation (Figure 4-F) has a mean of 0.59, a coefficient of variation of 17.42%, and slightly negative skewness (-0.11), indicating a concentration of values with the occurrence of lower extremes.

Figure 4

Sliding DFA of streamflow, mean temperature, and precipitation in the Licungo River Basin from 2002 to 2022 with their respective histograms



Notes: 1 – In the histograms, CV denotes the coefficient of variation and As denotes the skewness coefficient. 2 – The horizontal dashed line denotes $\alpha = 0.5$. 3 – The exponents α were computed using $w = 365$ days.
Source: Prepared by the authors.

Overall, the application of sliding DFA allowed for a deeper interpretation of the temporal memory of the analyzed variables. The mean values of the exponent α_{DFA} indicate strong persistence for both streamflow and temperature, suggesting that these series exhibit long-term dependence, in which past conditions significantly influence future behavior. This result is consistent with the literature, which associates α values close to or greater than 1 with systems exhibiting long-range memory and strong temporal structure (Kantelhardt *et al.*, 2002; Peng *et al.*, 1994). In contrast, precipitation showed α values close to the threshold between randomness and weak persistence, reflecting the intermittent and highly stochastic nature of tropical rainfall. Studies applying dimensionality reduction techniques and multivariate analysis to environmental time series highlight that this distinction between persistent and near-random variables is essential for selecting appropriate predictive models, especially in systems subject to high climatic variability (Campo-Bescós *et al.*, 2013).

3.4 SLIDING BIVARIATE CORRELATION

Figure 5 presents the temporal and multiscale evolution of the detrended cross-correlation coefficient $\rho_{DCCA}(n)$, obtained using sliding windows with length $w=365$ days, among the analyzed hydroclimatic variables. The horizontal axis represents time (2003 to 2021), while the vertical axis corresponds to the time scale n, in days ($4 \leq n \leq 90$). This representation allows the identification of variations in correlation intensity over time and across different scales, as well as periods that deviate from the dominant pattern.

In the streamflow–temperature panel (Figure 5-A), the cross-correlation is predominantly weak to moderate throughout most of the analyzed period. However, variations in the intensity of this correlation are observed in specific time intervals, with localized regions of weakening characterized by values close to zero. These occurrences are more evident around the periods from 2006 to 2008, 2011 to 2013, and in years after 2016, depending on the time scale considered, indicating intermittent reductions in the association between streamflow and temperature.

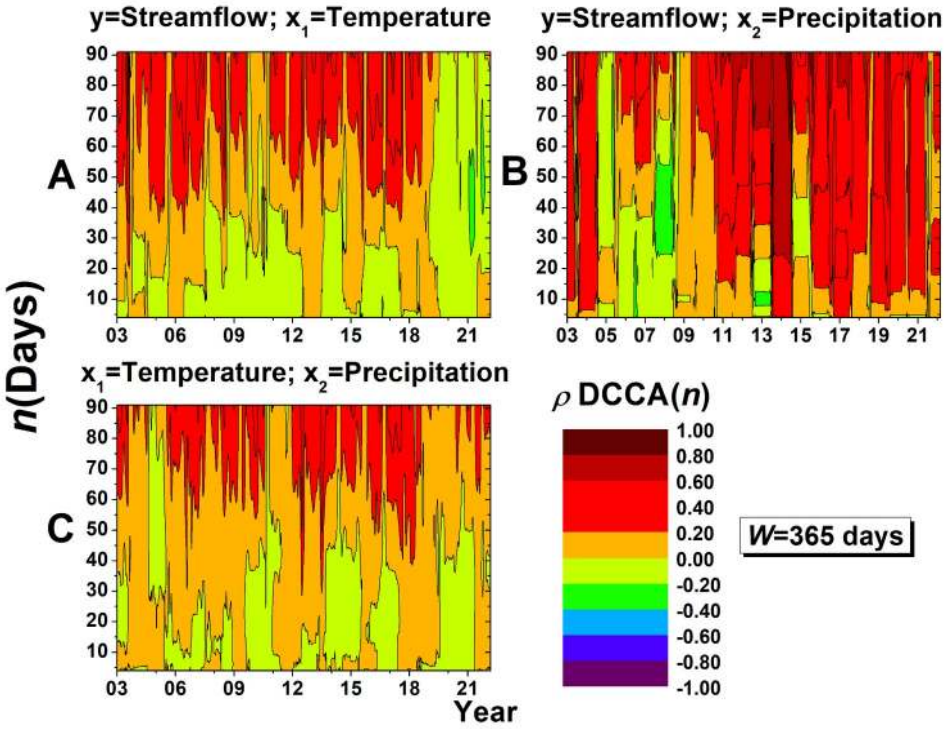
Complementarily, for the streamflow–precipitation pair (Figure 5-B), a dominant pattern of strong to very strong correlation is observed across much of the time?scale domain. Nevertheless, there are variations in the intensity of this relationship, with localized regions of attenuation where the correlation decreases to moderate levels. These patterns are more evident at the beginning of the series, approximately between 2004 and 2006, and, sporadically, in intervals around 2012 and 2017, reflecting temporal fluctuations in the dependence between precipitation and streamflow.

In turn, for the temperature–precipitation pair (Figure 5-C), a predominance of very weak to weak correlations is observed throughout most of the analyzed period. However, localized regions of increased correlation are identified, reaching moderate and, occasionally, higher levels, particularly during the intervals 2005–2007, 2010–2012, and in segments close to 2018, with these occurrences restricted to specific time scales.

Overall, periods that deviate from the dominant correlation pattern do not occur continuously but rather appear as localized episodes that depend on the analyzed time scale. This behavior highlights the non-stationary nature of interactions among hydroclimatic variables and underscores the usefulness of the sliding window approach for identifying variations in the correlation structure across the time?scale domain, consistent with the findings of (Doria *et al.*, 2025).

Figure 5

Sliding bivariate correlation $\left(\rho_{DCCA(n)}\right)$ *between time series of the Licungo River Basin from 2002 to 2022*



Notes: 1 – y denotes streamflow, x_1 temperature, and x_2 precipitation. 2 – The sliding correlation was computed using a window of $w = 365$ days.
Source: Prepared by the authors.

In this context, the analysis of sliding bivariate correlation using the DCCA coefficient reveals a consistent coupling between precipitation and streamflow across multiple time scales, particularly between 20 and 90 days, indicating that streamflow responds in an integrated manner to accumulated rainfall. This pattern is consistent with basins characterized by lower groundwater storage capacity and greater contribution from surface runoff. The moderate correlation observed between temperature and streamflow suggests an indirect influence of this variable, possibly mediated by evapotranspiration and water balance processes, while the relationship between temperature and precipitation appears more unstable and intermittent over time and across the analyzed scales.

Similar results have been reported in studies investigating the coevolution of climatic and hydrological variables in semi-arid and tropical regions of Southern Africa, in which stronger correlations emerge at intermediate scales, reflecting the combined influence of local processes and regional climatic forcing (Southworth *et al.*, 2018).

3.5 SLIDING MULTIPLE CROSS-CORRELATION

Figure 6 presents the time–scale map of the detrended multiple cross-correlation coefficient $DMC_x^2(n)$, estimated using sliding windows with length $w = 365$ days, considering time (years) on the horizontal axis and time scales n on the vertical axis. In general, most of the time?scale domain is characterized by values classified as very weak $(0.0 - 0.2)$, indicating low multiple dependence among streamflow, temperature, and precipitation over the analyzed period.

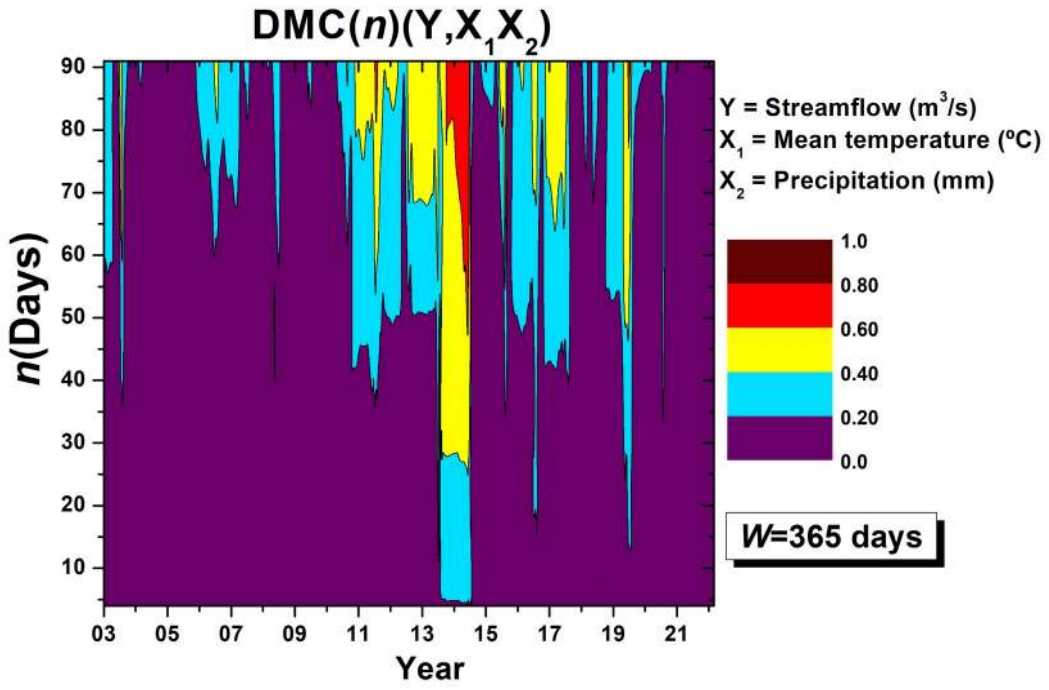
At shorter time scales, the coefficient $DMC_x^2(n)$ remains predominantly within the very weak range throughout almost the entire time interval, with rare occurrences of weak correlation. This pattern indicates that, at scales of a few days to a few weeks, the joint interaction among the variables is limited when assessed through detrended multiple cross-correlation. As the time scale increases, greater variability in $DMC_x^2(n)$ is observed over time. At intermediate scales, although the very weak classification still predominates, localized regions of weak to moderate correlation emerge, particularly during the period around 2012 to 2014. These episodes indicate moments when the joint dependence among the variables becomes more pronounced at scales ranging from weeks to approximately two months.

In turn, at larger time scales, the behavior of $DMC_x^2(n)$ is marked by greater fragmentation over time. Sparse patches of weak to moderate correlation are observed throughout the series, along with an isolated episode of strong correlation around 2014. Outside these intervals, the values predominantly return to the very weak range, reinforcing the episodic nature of multiple dependence at longer time scales.

In summary, the scale-based analysis shows that the detrended multiple cross-correlation among streamflow, temperature, and precipitation is predominantly very weak, regardless of the scale considered. However, specific years?particularly within the approximate interval from 2012 to 2014 deviate from this pattern by exhibiting increases in $DMC_x^2(n)$ to weak, moderate, and occasionally strong levels, especially at intermediate and larger scales. These results highlight the non-stationary and episodic nature of the multiple dependence among the analyzed variables.

Figure 6

Sliding Multiple Correlation $DMC(n)$ of the Licungo River Basin from 2002 to 2022



Notes: 1 – Y denotes streamflow, X_1 mean temperature, and X_2 precipitation. 2 – The sliding multiple correlation was computed using a window of $w = 365$ days.
Source: Prepared by the authors.

Figure 7 presents the temporal evolution of the detrended multiple cross-correlation coefficient $DMC_x^2(n)$ for specific scales ($n = 7$, 15, 30, and 90 days), calculated from the same dataset used in the time?scale analysis (Figure 6). This representation allows for a more detailed analysis of the coefficient behavior at selected scales, facilitating the identification of temporal variations and periods that deviate from the overall pattern observed in the complete map.

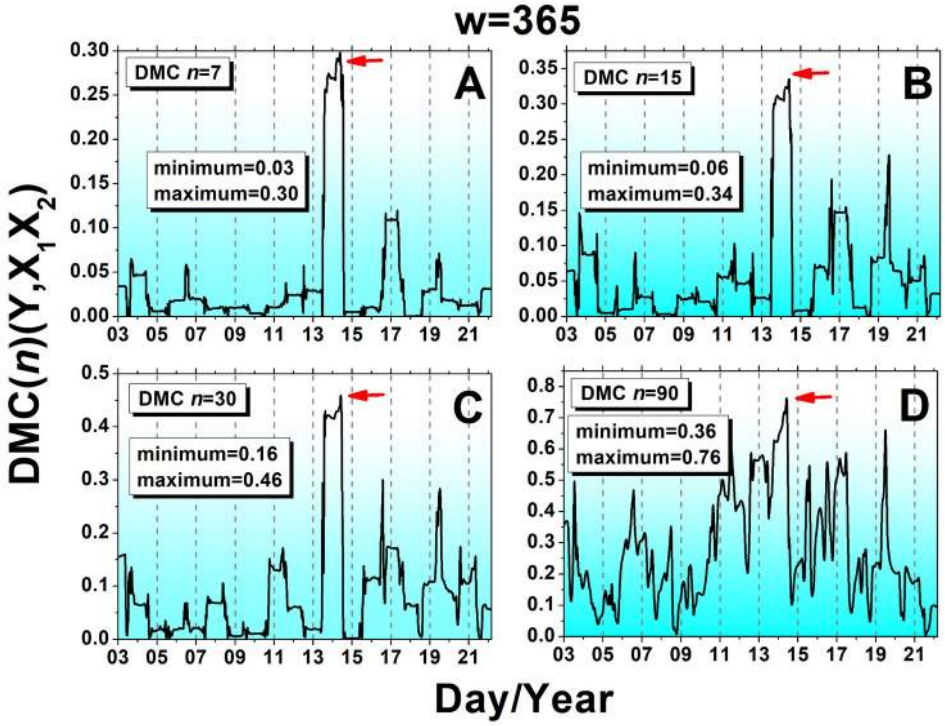
At smaller scales ($n = 7$ and $n = 15$ days), values classified as very weak to weak predominate, with occasional increases mainly concentrated in the period 2012–2014. As the scale increases, a gradual intensification of multiple dependence is observed. At the intermediate scale ($n = 30$ days), more pronounced episodes emerge, with values ranging from weak to moderate. At the longest scale ($n = 90$ days), multiple dependence becomes more evident, reaching moderate to strong levels in specific periods, again particularly during 2012–2014 (Figure 7). These results are consistent with the previously presented time?scale

analysis and reinforce the episodic and scale-dependent nature of the multiple cross-correlation among the analyzed variables.

From a multivariate perspective, the incorporation of the Multiple Cross-Correlation (DMC) coefficient allows for an integrated assessment of the simultaneous influence of precipitation and temperature on streamflow, overcoming the limitations inherent to strictly bivariate analyses. The DMC, based on the generalization of the ρ_{DCCA} coefficient for multiple series, synthesizes in a single index the intensity of climate?hydrological coupling across different time scales. Recent studies show that this coefficient is highly sensitive to the scale of analysis, revealing weaker correlations in short windows and more robust coupling at monthly or quarterly scales, when the cumulative effects of physical processes become more evident (Brito *et al.*, 2019; Zebende & Silva–Filho., 2018).

Figure 7

Sliding multiple cross-correlation DMC_x^2 for specific scales ($n=7$, $n=15$, $n=30$, and $n=90$ days) of the Licungo River Basin from 2002 to 2022



Note: The sliding multiple correlation was computed using a window of $w=365$ days.
Source: Prepared by the authors.

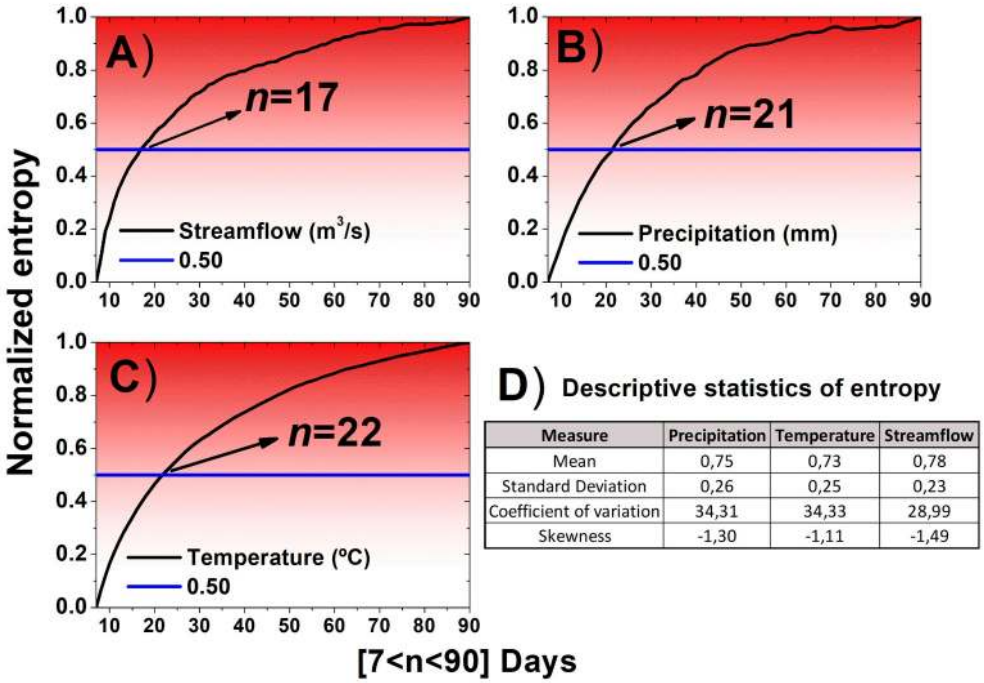
In the context of the Licungo Basin, the sliding DMC results indicated periods of intensified joint climatic control over streamflow, notably between 2013 and 2016, when high

coefficient values were observed in windows ranging from 30 to 90 days. This behavior suggests greater synchronization between temperature, precipitation, and hydrological response, possibly associated with the occurrence of regional climatic anomalies. Applications of DMC in African and tropical regions (Afuecheta; Omar, 2021) report similar patterns, in which peaks of the multiple coefficient coincide with episodes of large-scale climate variability, reinforcing the usefulness of the method for identifying distinct hydrological regimes.

3.6 NORMALIZED FASTAPEN ENTROPY

Figure 8

Normalized entropy of streamflow, mean temperature, and precipitation in the Licungo River Basin from 2002 to 2022 for different time scales n



Measure	Precipitation	Temperature	Streamflow
Mean	0,75	0,73	0,78
Standard Deviation	0,26	0,25	0,23
Coefficient of variation	34,31	34,33	28,99
Skewness	-1,30	-1,11	-1,49

Notes: 1 – The horizontal blue line denotes entropy equal to 0.50 (moderate entropy). 2 – The entropy of the evaluated time series was defined for scales ranging from 7 to 90 days inclusive. 3 – The table presents the descriptive statistics considering all evaluated scales.
Source: Prepared by the authors.

Figure 8 allows the evaluation of the predictability of hydroclimatic series (streamflow, precipitation, and temperature) through normalized FASTApEn entropy, calculated for time scales in the range $7<n<90$ days. In general, a consistent behavior is observed among the

variables: entropy increases with scale, indicating a systematic reduction in predictability as one moves from shorter to longer time scales.

The streamflow series (Figure 8-A) presents a mean entropy of 0.78 (standard deviation = 0.23; CV = 28.99%), with the curve crossing the 0.50 threshold at approximately $n \approx 17$ days. Thus, scales below ~ 17 days exhibit higher relative predictability, while at larger scales a progressive increase in entropy is observed, characterizing a transition to regimes of lower predictability. The lower coefficient of variation among the variables indicates a smoother transition for streamflow. All series present negative skewness, indicating a greater concentration of entropy values above the mean.

Precipitation (Figure 8-B) (mean entropy = 0.75; standard deviation = 0.26; CV = 34.31%) shows greater sensitivity to scale, with a more pronounced increase in entropy and crossing the 0.50 threshold at around $n \approx 21$ days, exceeding 0.70 at scales greater than approximately 30 days. This behavior indicates a significant reduction in predictability at monthly scales.

Temperature (Figure 8-C) (mean entropy = 0.73; standard deviation = 0.25; CV = 34.33%) exhibits a similar pattern, with the 0.50 threshold being reached at around $n \approx 22$ days and a progressive increase in entropy at larger scales. In practical terms, the results indicate that short-term forecasts (approximately 7–15 days) are more reliable, whereas forecasts at scales greater than 20–30 days present higher uncertainty, especially for precipitation.

Studies conducted in African basins show that entropy-based approaches can be used to optimize monitoring networks by prioritizing regions that maximize hydrological information gain (Tekleyohannes *et al.*, 2021). In this context, the results obtained for the Licungo Basin provide relevant support for improving hydrometeorological networks.

A normalized entropy value of 0.50 was adopted as a reference for moderate predictability. Values below this threshold indicate greater regularity and potential for operational forecasting, whereas values above it reflect higher uncertainty, requiring probabilistic approaches. These results provide support for optimizing monitoring systems and decision-making in the studied basin.

3.7 JOINT ANALYSIS

Our findings reinforce that hydroclimatic systems are intrinsically complex, nonlinear, and strongly influenced by multiple climatic and environmental factors, resulting in high temporal variability and uncertainty in hydrological processes (Badou *et al.*, 2017; Ilunga,

2017). In particular, the relationship between precipitation and streamflow has been widely documented, showing significant dependencies and hydrological responses sensitive to climate change (Badou *et al.*, 2017). Additionally, entropy has been used as a robust measure of uncertainty and complexity in these systems, enabling the characterization of variability and hydrological resilience (Ilunga, 2017; Ilunga; Singh, 2015).

From an integrated perspective, the results indicate that the hydroclimatic system of the Licungo Basin is partially coupled: precipitation acts as the main external forcing, streamflow responds with long-term memory, and temperature plays a modulating role. Multivariate analysis via DMC reinforces this interpretation by showing that the combined effect of meteorological variables on streamflow is not constant over time, but rather dependent on the time scale and the prevailing climatic regime. This configuration implies that forecasting and management strategies should explicitly consider the scale of interest, combining univariate, bivariate, and multivariate analyses for a more accurate representation of hydrological dynamics.

Despite these advances, the literature still lacks approaches capable of explicitly capturing long-range dependencies and multiscale dynamics in hydroclimatic time series. In this context, the integrated application of methods such as DFA, DCCA, DMC, and entropy, as adopted in this study, represents a relevant methodological advance, as it enables the simultaneous investigation of temporal memory, cross-correlation, and predictability across different scales. This approach is particularly suitable for basins in tropical regions, where hydroclimatic variability is high and processes are strongly influenced by extreme events.

4 RESEARCH LIMITATIONS

Although the results obtained are robust and relevant for understanding the hydroclimatic dynamics of the Licungo River Basin, some limitations should be considered. The analysis is based on a single hydrometric station, which may not fully represent the spatial variability of the basin, in addition to the presence of data gaps, treated through imputation, which may introduce minor uncertainties. Additionally, the use of a fixed sliding window ($w = 365$ days) may smooth short-term variations.

The methods employed (DFA, DCCA, DMC, and FastApEn) identify patterns of dependence and multiscale variability but do not allow the inference of direct causal relationships. Therefore, the results should be interpreted as evidence of statistical interdependence, possibly associated with physical processes of the hydrological cycle?such

as surface runoff, water storage, and evapotranspiration. Thus, the findings should be understood as indications of statistical interdependence linked to hydrological processes, including runoff, water storage, and evapotranspiration. Accordingly, the integration of process-based approaches is recommended for future studies.

5 CONCLUSIONS

The results of this study confirm that the proposed objective was achieved, allowing for an integrated and multiscale characterization of the hydroclimatic dynamics of the Licungo River Basin. The system exhibits complex and non-stationary behavior, characterized by high rainfall variability, strong seasonality, and hydrological responses sensitive to extreme events. The exploratory analysis indicated that streamflow follows precipitation peaks, reflecting the predominance of surface runoff, while temperature shows a more stable behavior, with a slight warming trend in the recent period.

The multiscale approach adopted, combining sliding descriptive statistics, DFA, DCCA, DMC, and entropy, allowed the identification of fundamental properties of the time series. The results showed that streamflow exhibits long-range memory, precipitation plays a dominant role in hydrological dynamics, and temperature acts as a modulating variable. Correlation analyses revealed strong coupling between precipitation and streamflow, moderate dependence between temperature and streamflow, and a weaker relationship between temperature and precipitation. Additionally, entropy analysis indicated a reduction in predictability at scales greater than approximately 20 days, reinforcing the multiscale and non-stationary nature of the system.

Taken together, the results demonstrate that the hydroclimatic dynamics of the basin are governed by complex interactions, dependent on the time scale and strongly influenced by extreme events. These findings provide relevant support for improving hydrometeorological monitoring, hydrological modeling, and water resource management, especially in tropical regions with high climatic variability.

For future work, it is recommended to expand the database, incorporate additional environmental variables, and integrate statistical approaches with process-based models, including machine learning techniques, in order to enhance predictive capacity and the understanding of the mechanisms governing the system. Additionally, the comparative application of the methodology to other basins in Mozambique appears promising for assessing the generality of the identified patterns, contributing to the strengthening of

technical support for the formulation of public policies for water resource management and the mitigation of hydrological risks.

ACKNOWLEDGMENTS

The authors would like to thank the State University of Feira de Santana (UEFS) for financial support.

REFERENCES

ACAPS. (2019). *Mozambique: Tropical Cyclone Idai – Briefing Note*. ACAPS / ReliefWeb. https://reliefweb.int/disaster/tc-2019-000021-moz

Afuecheta, E., & Omar, M. H. (2021). Characterization of variability and trends in daily precipitation and temperature extremes in the Horn of Africa. *Climate Risk Management*, *32*, 100295.

Azami, J., H.; Escudero. (2016). Amplitude- and frequency-based permutation entropy for time-series analysis. *IEEE Signal Processing Letters*, *23*(5), 610–614.

Badou, D. F., Kapangaziwiri, E., Diekkrüger, B., Hounkpè, J., & Afouda, A. (2017). Evaluation of recent hydro-climatic changes in four tributaries of the niger river basin (West Africa). *Hydrological Sciences Journal*, *62*(5), 715–728. https://doi.org/10.1080/02626667.2016.1250898

Brito, A. de A., Araújo, H. A. de, & Zebende, G. F. (2019). Detrended multiple cross-correlation coefficient applied to solar radiation, air temperature and relative humidity. *Scientific Reports*, *9*, 19764.

Campo-Bescós, M. A., Muñoz-Carpena, R., Southworth, J., Zhu, L., Waylen, P. R., & Bunting, E. (2013). Combined spatial and temporal effects of environmental controls on long-term monthly NDVI in the Southern Africa Savanna. *Remote Sensing*, *5*, 6513–6538.

Cea, L., Álvarez, M., & Puertas, J. (2022). Estimation of flood-exposed population in data-scarce regions combining satellite imagery and high resolution hydrological-hydraulic modelling: A case study in the licungo basin (Mozambique). *Journal of Hydrology: Regional Studies*, *44*, 101247. https://doi.org/10.1016/j.ejrh.2022.101247

Costa, N., Silva, C., & Ferreira, P. (2019). Long-range behaviour and correlation in DFA and DCCA analysis of cryptocurrencies. *International Journal of Financial Studies*, *7*(3), 51. https://doi.org/10.3390/ijfs7030051

DNGRH. (2014). *Plano nacional de recursos hídricos: Prioridades 2012–2015* [Relatório Técnico]. Ministério das Obras Públicas, Habitação.

Doria, T. S. S., Guedes, E. F., Santos, E. C. O., & Silva Filho, A. M. (2025). Análise temporal de variáveis climatológicas com janelas deslizantes. *Revista Brasileira de Climatologia*,

37, 493–531.

Droogers, P., & Bouma, J. (2014). Simulation modelling for water governance in basins. *International Journal of Water Resources Development*, *30*(3), 475–494. https://doi.org/10.1080/07900627.2014.903771

Erler, A. R., Frey, S. K., Khader, O., dOrgeville, M., Park, Y., Hwang, H., Lapen, D. R., Peltier, W. R., & Sudicky, E. A. (2019). Evaluating climate change impacts on soil moisture and groundwater resources within a lake-affected region. *Water Resources Research*, *55*(10), 8142–8163. https://doi.org/10.1029/2018wr023822

Guedes, E. F., Silva Filho, A. M., & Zebende, G. F. (2021). Detrended multiple cross-correlation coefficient with sliding windows approach. *Physica A: Statistical Mechanics and Its Applications*, *574*, 125990. https://doi.org/10.1016/j.physa.2021.125990

Hakam, O., Ongoma, V., Beniaich, A., Meskour, B., El Kadi, M. A., Brouziyne, Y., Hssaisoune, M., Tairi, A., Labbaci, A., & Bouchaou, L. (2024). Assessment of the impact of climate change on argan tree in the Mediterranean GIAHS site, Morocco: Current and future distributions. *Modeling Earth Systems and Environment*, *10*(4), 5529–5552. https://doi.org/10.1007/s40808-024-02077-1

Hartmann, D. L. *et al.* (2013). Observations: Atmosphere and surface. In T. F. Stocker, D. Qin, G.-K. Plattner, M. Tignor, S. K. Allen, J. Boschung, A. Nauels, Y. Xia, V. Bex, & P. M. Midgley (Eds.), *Climate change 2013: The physical science basis. Contribution of working group i to the fifth assessment report of the intergovernmental panel on climate change* (pp. 159–254). Cambridge University Press. https://doi.org/10.1017/CBO9781107415324.008

Ilunga, M. (2017). Assessing catchment resilience using entropy associated with mean annual runoff for the upper vaal catchment in South Africa. *Entropy*, *19*, 147.

Ilunga, M. (2019). Shannon Entropy for Measuring Spatial Complexity Associated with mean annual runoff of tertiary catchments of the middle vaal basin in South Africa. *Entropy*, *21*, 366.

Ilunga, M., & Singh, V. P. (2015). Measuring spatial variability of land use associated with hydrological impact in urbanised quaternary catchments using entropy. *Water SA*, *41*(1), 41–50. https://doi.org/10.4314/wsa.v41i1.7

International Federation of Red Cross and Red Crescent Societies. (2015). *Emergency plan of action (EPoA): Mozambique floods, january 2015*. International Federation of Red Cross; Red Crescent Societies (IFRC). https://adore.ifrc.org/Download.aspx?FileId=70259

Juizo, D., & Liden, R. (2010). Modeling for transboundary water resources planning and allocation: The case of southern africa. *Hydrology and Earth System Sciences*, *14*(11), 2343–2354. https://doi.org/10.5194/hess-14-2343-2010

Kantelhardt, J. W., Zschiegner, S. A., Koscielny-Bunde, E., Havlin, S., Bunde, A., & Stanley, H. E. (2002). Multifractal detrended fluctuation analysis of nonstationary time series.

Physica A: Statistical Mechanics and Its Applications, *316*(1–4), 87–114. https://doi.org/10.1016/S0378-4371(02)01383-3

Kapur, J. N., & Kesavan, H. K. (1992). Entropy optimization principles and their applications. In *Entropy and energy dissipation in water resources* (pp. 3–20). Springer.

Köplin, N., Schädler, B., Viviroli, D., & Weingartner, R. (2012). Relating climate change signals and physiographic catchment properties to clustered hydrological response types. *Hydrology and Earth System Sciences*, *16*(7), 2267–2283. https://doi.org/10.5194/hess-16-2267-2012

Li, V. P. ;. M., D.; Singh. (2018). Entropy theory in hydrologic science and engineering. *Water Resources Research*, *54*(2), 1031–1058.

Liang, Z. ;. W., C.; Xu. (2020). Entropy-based analysis for ecological time series: Diversity and stability in complex systems. *Ecological Modelling*, *4020*, 108994.

Muchangos, A. dos. (1999). *Moçambique: Paisagens e regiões naturais*. Tipografia Globo.

NASA Earth Observatory. (2015). *Flooding in Mozambique (january 2015)*. https://science.nasa.gov/earth/earth-observatory/flooding-in-mozambique-85145/

New, M., Lister, D., Hulme, M., & Makin, I. (2002). A high-resolution data set of surface climate over global land areas. *Climate Research*, *21*, 1–25. https://doi.org/10.3354/cr021001

Peng, C.-K., Buldyrev, S., Havlin, S., Simons, M., Stanley, H., & Goldberger, A. (1994). Mosaic organization of DNA nucleotides. *Physical Review. E, Statistical Physics, Plasmas, Fluids, and Related Interdisciplinary Topics*, *49*, 1685–1689. https://doi.org/10.1103/PhysRevE.49.1685

Pereira, A. R. B., Costa, C. T. F. da, Firmino, P. R. A., Studart, T. M. de C., & Oliveira, C. W. (2024). Preenchimento de falhas em séries de dados meteorológicos de estações automáticas. *Revista Brasileira de Climatologia*, *35*, 22–44. https://ojs.ufgd.edu.br/index.php/rbclima

Pincus, S. M. (1991). (1991). Approximate entropy as a measure of system complexity. *Proceedings of the National Academy of Sciences*, *88*(6), 2297–2301. https://doi.org/10.1073/pnas.88.6.2297

Podobnik, B., & Stanley, H. (2008). Detrended Cross-Correlation Analysis: A New Method for Analyzing Two Nonstationary Time Series. *Physical Review Letters*, *100*, 084102. https://doi.org/10.1103/PhysRevLett.100.084102

Ribas Junior, N. S., Guedes, E. F., Castro, A. P. N. de, & Silva Filho, A. M. (2026). The influence of non-oceanic forces on the mean sea level of the brazilian coast: A bivariate and multivariate approach. *Scientific Reports*. https://doi.org/10.1038/s41598-026-39554-9

Ribas Junior, N. S., Guedes, E. F., Dias, R., & Silva Filho, A. M. (2025). Sea level on the brazilian coast: A sliding windows approach. *Journal of South American Earth Sciences*,

153, 105360. https://doi.org/10.1016/j.jsames.2025.105360

Richman, J. S., & Moorman, J. R. (2000). Physiological time-series analysis using approximate entropy and sample entropy. *American Journal of Physiology-Heart and Circulatory Physiology*, *278*(6), H2039–H2049.

Santos, E. C. O., Guedes, E. F., Zebende, G. F., & Silva Filho, A. M. (2022). Autocorrelation of wind speed: A sliding window approach. *Physica A: Statistical Mechanics and Its Applications*, *607*, 128213. https://doi.org/10.1016/j.physa.2022.128213

Shannon, C. E. (1948). A mathematical theory of communication. *Bell System Technical Journal*, *27*(3), 379–423. https://doi.org/10.1002/j.1538-7305.1948.tb01338.x

Silva Filho, A. M. da, Castro, A. P. N., & Guedes, E. F. (2026). Multifractal detrended multiple cross-correlation coefficient qDMC. *Physica A: Statistical Mechanics and Its Applications*, *689*, 131424. https://doi.org/10.1016/j.physa.2026.131424

Silva Filho, A. M., Zebende, G. F., & Guedes, E. F. (2021). Analysis of intentional lethal violent crimes: A sliding windows approach. *Physica A: Statistical Mechanics and Its Applications*, *567*, 125653. https://doi.org/10.1016/j.physa.2020.125653

Singh, V. P. (2013). *Entropy theory and its application in environmental and water engineering*. John Wiley & Sons.

Southworth, J., Bunting, E., Zhu, L., Ryan, S. J., Herrero, H. V., Waylen, P., *et al.* (2018). Using a coupled dynamic factor – random forest analysis (DFRFA) to reveal drivers of spatiotemporal heterogeneity in the semi-arid regions of southern Africa. *PLOS ONE*, *13*(12), e0208400.

Tekleyohannes, M., Grum, B., Abebe, N., & Abebe, B. A. (2021). Optimization of rain gauge network using multi-criteria decision analysis and entropy approaches: Case of tekeze river basin, northwestern Ethiopia. *Theoretical and Applied Climatology*, *145*, 159–174.

Tibangayuka, N., Mulungu, D. M. M., & Izdori, F. (2025). Evaluating future climate-driven changes in agricultural water resilience: Insights from CMIP6 model simulations for the Kagera River sub-basin. *Journal of Environmental Management*, *378*, 124745. https://doi.org/10.1016/j.jenvman.2025.124745

Toledo, O. C., Silva Filho, A. M. da, Silva, A. B., & Zebende, G. F. (2022). Temporal analysis of the flows of the rivers that form the hydrographic basin of Moquegua Peru. *Fluctuation and Noise Letters*, *21*(6). https://doi.org/10.1142/S0219477522500596

Tomčala, J. (2018). Acceleration of time series entropy algorithms. *The Journal of Supercomputing*, *75*(3), 1443–1454. https://doi.org/10.1007/s11227-018-2657-2

Viviroli, D., Archer, D. R., Buytaert, W., Fowler, H. J., Greenwood, G. B., Hamlet, A. F., Huang, Y., Koboltschnig, G., Litaor, M. I., Lopez-Moreno, J. I., Lorentz, S., Schädler, B., Schreier, H., Schwaiger, K., Vuille, M., & Woods, R. (2011). Climate change and mountain water resources: Overview and recommendations for research, management and policy.

Hydrology and Earth System Sciences, *15*(2), 471–504. https://doi.org/10.5194/hess-15-471-2011

Zebende, G. F., & Silva–Filho., A. M. da. (2018). Detrended Multiple Cross-Correlation Coefficient. *Physica A*, *510*, 91–97.

Zebende, G. F., Fernandez, B. F., & Pereira, M. G. (2016). Analysis of the variability in the sdB star KIC 10670103; DFA approach. *Monthly Notices of the Royal Astronomical Society*, *464*(3), 2638–2642. https://doi.org/10.1093/mnras/stw2611

Zebende, G. Figueira. (2011). DCCA cross-correlation coefficient: Quantifying level of cross-correlation. *Physica A*, *390*, 614–618.